Identification of 40S ribosomal protein S8 as a novel biomarker for alcohol-associated hepatocellular carcinoma using weighted gene co-expression network analysis

NINGRUI BI[1*], YUANMEI SUN[2,3*], SHAN LEI[2,3*], ZHIRUI ZENG[2,3], YAN ZHANG[3], CHENGYI SUN[1] and CHAO YU[1]

[1]Department of Liver-Biliary Surgery, Affiliated Hospital of Guizhou Medical University;
[2]Guizhou Provincial Key Laboratory of Pathogenesis and Drug Research on Common Chronic Diseases;
[3]Department of Physiology, School of Basic Medicine, Guizhou Medical University, Guiyang, Guizhou 550009, P.R. China

Received August 8, 2019; Accepted January 28, 2020

DOI: 10.3892/or.2020.7634

Abstract. Alcohol-associated hepatocellular carcinoma (HCC) is a subtype of HCC with poor prognosis. The present study aimed to identify key biomarkers for alcohol-associated HCC. The gene data profiles and corresponding clinical traits of patients with alcohol-associated HCC were downloaded from The Cancer Genome Atlas (TCGA) database. Firstly, good genes and good samples were identified, which were subsequently used to conduct weighted gene co-expression network analysis (WGCNA). Hub genes in the significant modules were selected following Gene Ontology (GO) and Kyoto Encyclopedia of Genes and Genomes (KEGG) pathway enrichment analyses, and from constructing a protein-protein interaction (PPI) network. Real hub genes among hub genes were determined following progression, survival analysis and gene set enrichment analysis (GSEA), as well as reverse transcription-quantitative PCR and immunohistochemical staining of non-alcohol- and alcohol-associated HCC samples. In total, 64 good samples of alcohol-associated HCC with height score <160 were selected, from which 15,195 good genes were identified and used to conduct WGCNA; 8 gene co-expressed modules were identified using WGCNA, while 3 modules (including pink, magenta and turquoise) were significantly associated with Child-Pugh score, T-stage and body weight. Following GO and KEGG analysis and construction of the PPI network, a total of 30 hub genes were identified in the aforementioned 3 gene co-expressed modules, while 16 hub genes (including AURKB, BUB1, BUB1B, CCNB1, CCNB2, CDC20, CDCA8, CDK1, PLK1, RPS5, RPS7, RPS8, RPS14, RPS27, RPSA and TOP2A) were associated with the development of alcohol-associated HCC, and had a significant prognosis value. Among these genes, only RPS8 was highly expressed in alcohol-associated HCC, but not in non-alcohol-associated HCC, while RPS5 was not significantly associated in either alcohol- or non-alcohol-associated HCC. GSEA demonstrated that 10 pathways, including RNA polymerase and ribosome pathways were enriched in alcohol-associated HCC samples where RPS8 was highly expressed. Taken together, the results of the present study demonstrate that RPS8 may be a novel biomarker for the diagnosis of patients with alcohol-associated HCC.

Introduction

Human hepatocellular carcinoma (HCC) is a common malignancy of the digestive system and is the third leading cause of tumor-related mortality (>780,000 cases per year) worldwide according to data from 2018 (1). Alcohol consumption, hepatitis B virus (HBV) and hepatitis C virus (HCV) infection are known to be causative factors of HCC (2). In recent years, the morbidity rate from alcohol-associated HCC has increased in developed countries (accounting for 40% cases of HCC), as well as in China (accounting for 28% cases of HCC) (3). A previous study has demonstrated that in the human body, ethanol is metabolized into acetaldehyde by alcohol dehydrogenase (4) and acetaldehyde exerts a carcinogenic effect by binding to 2'-deoxyguanosine in hepatocyte DNA and causing DNA mutations (5). During metabolism, reactive oxygen species accumulate and promote further DNA damage, including chain interruption and heterogeneous interconversion (6). However, the molecular mechanism of alcohol-associated HCC is yet to be elucidated, thus, identification of key genes associated with the development of alcohol-associated HCC may increase these mechanisms, as well as identifying potential biomarkers and targets for diagnosis and treatment, respectively.

Correspondence to: Professor Chengyi Sun or Professor Chao Yu, Department of Liver-Biliary Surgery, Affiliated Hospital of Guizhou Medical University, 28 Guiyi Road, Guiyang, Guizhou 550009, P.R. China
E-mail: chengyisun2014@163.com
E-mail: yuchao2002@gmc.edu.cn

*Contributed equally

Key words: hepatocellular carcinoma, weight gene co-expression network analysis, hub genes, 40S ribosomal protein S8

Microarray and RNA-sequencing (RNA-seq) technology are valuable tools for monitoring genome-wide changes in gene expression. In previous studies, bioinformatics analysis of microarray and RNA-seq gene data profiles identified key onco-genes, such as cell division cycle 20 and cell division cycle associated 5 involved in the prognosis of HCC (7,8). In a preliminary bioinformatics study, Wu *et al* (9) identified 12 genes, including non-SMC condensin I complex subunit G and TTK protein kinase that were associated with the progression of HCC. In addition, Pan *et al* (10) revealed that micro(mi) RNA-15b-5p serves an oncogenic role in HCC. Through the investigation of miRNA-mRNA regulatory pathways, Lou *et al* (11) revealed 36 differentially expressed miRNAs, including miR-93-5p and miR-106-5p, which increased the activation of mitogen-activated protein kinase 8 pathway and promoted the development of HCC. Furthermore, Yin *et al* (12) used weighted gene co-expression network analysis (WGCNA) to identify 13 genes, including cyclin-dependent kinase 1 and topoisomerase 2α which were found to promote the development of HCC.

In the present study, RPS8 was found to be highly expressed in alcohol-associated HCC and associated with tumor progression, but not with non-alcohol-associated HCC. Thus, RPS8 may be a novel and specific biomarker and potential therapeutic target for alcohol-associated HCC.

Materials and methods

Data collection and processing. Data of patients with HCC and with a history of alcohol consumption were downloaded from TCGA database; a total of 68 alcohol-associated HCC tissue samples and the corresponding patient clinical traits including age, Child-Pugh score, T-stage, patient status (dead or alive) and body weight were obtained from The University of California Santa Cruz (https://xenabrowser.net/data-pages/). The gene matrix of the 68 profiles was normalized using the limma package (version 3.10; http://www.bioconductor.org/packages/release/bioc/html/limma.html) and transferred as log2 (fragments per kilobase of exon model per million reads mapped; FPKM+1). Before conducting WGCNA, the probes without gene symbols, and the genes with a mean expression level <0.5 were removed. Concurrently, the hierarchical cluster (Hclust) algorithm (version 3.4.1; http://web.mit.edu/~r/current/arch/amd64_linux26/lib/R/library/stats/html/hclust.html) was performed to cluster the samples according to the gene expression of the whole genome and to detect outliers. Then, the height (a score for evaluating the mean dissimilarity) of each sample was calculated and the threshold for identifying outlier samples was set at 160. The remaining 15,195 genes and 64 samples were regarded as 'good genes' and 'good samples'.

WGCNA. Good samples and good genes were used to conduct WGCNA, and the WGCNA network was constructed using the R package 'WGCNA' (version: 1.68; R Project Organization; https://cran.r-project.org/web/packages/ WGCNA/index.html). First, the gradient method was employed to measure the independence and average connectivity degree of the different modules with different power values (1-20). A degree of scale independence (≥0.85) and low mean connectivity (~0.0) were selected as the threshold obtain power values of 1-20, following which module construction was performed. The minimum number of genes in each co-expressed gene module was set as 100. When the comparability of module eigengenes between two modules were <0.25, the modules were merged.

Identification of clinically significant modules and module core genes. Following WGCNA, the different module eigengenes and their corresponding clinical traits were correlated using Pearson's correlation analysis; five clinical traits were studied in the present study, including age, Child-Pugh score, T-stage, patient status (dead or alive) and weight. P<0.05 was used as the threshold for a significant association between gene modules and clinical traits. According to the requirements of the WGCNA algorithm, the result from the grey module is invalid, as the genes in the module are not co-expressed (13). Gene module genes with a module membership >0.8 were determined to be module core genes.

GO and KEGG pathway enrichment analysis. Module core genes were used to perform GO and KEGG analyses. The core gene data were uploaded to the Database for Annotation, Visualization and Integrated Discovery (DAVID) v6.8 (http://david-d.ncifcrf.gov/). The results of GO and KEGG analysis were exported as .txt files and visualized using R software (version: 3.5.3; R Project Organization; https://www.r-project.org/). P<0.05 was used to indicate a statistically significant difference.

Construction of the PPI network. The core gene data were uploaded to the Search Tool for the Retrival of Interacting Genes/Proteins (STRING) online database (http://string-db.org). The node and edge information were exported as .txt files and visualized using Cytoscape software (version, 3.7.2; The Cytoscape Consoritum; https://cytoscape.org/). The Cytohub plug-in was used to analyze the degree score; genes with the top ten degree scores were identified as hub genes and used to construct a PPI sub-network.

Progression and survival analysis. The gene expression data of the hub genes and the tumor grade were imported into SPSS v20.0 (IBM Corp). The effect of hub gene expression on the progression of alcohol-associated HCC was analyzed using Pearson's correlation analysis. TCGA data from patients with alcohol-associated were divided into two groups according to the mean expression levels of the hub genes, and Kaplan-Meier survival analysis was used to detect the prognostic values of these genes.

Tissue samples. In total, 30 pairs of alcohol-associated HCC and adjacent normal tissues were provided by patients with a long history of alcohol consumption; 30 pairs of non-alcohol-associated HCC tissues and their adjacent normal tissue samples were also donated by patients with HCC, who did not consume alcohol or consumed low levels (which failed to meet the criteria for a long history of alcohol consumption). The criteria for a long history of alcohol consumption were as follows: i) History of drinking >5 years; and ii) an average alcohol consumption >40 ml per day in men, and >20 ml per day in women. There were 23 patients with HBV infection and 4 patients with HCV infection in both the alcohol- and the

non-alcohol-associated HCC group; in addition, there were 3 patients in both groups, which had neither HBV nor HCV infection. This was used to group the two sets of patients according to infection status (HBV, HCV or not infected), as this can affect expression levels of genes. The tissues were collected between March 2017 and June 2019. The mean age of patients with alcohol-associated HCC was 55.2±7.4 years (range, 39-63; with 13 females and 17 male), while the mean age of the patients with non-alcohol associated HCC was 53.1±9.2 years (range, 36-65; with 14 females and 16 males). All samples were obtained from the Affiliated Hospital of Guizhou Medical University, (Guizhou, China) and the study was approved by the Ethics Committee of Guizhou Medical University and performed in accordance with the Declaration of Helsinki. Informed consent was provided from all patients.

Reverse transcription-quantitative PCR (RT-qPCR). Total RNA was extracted from non-alcohol- and alcohol-associated HCC tissues using TRIzol® reagent (Invitrogen; Thermo Fisher Scientific, Inc.), and reverse transcribed into cDNA using the First Strand cDNA Synthesis kit (Shanghai Yeasen Biotechnology Co., Ltd.). under the following conditions: 37˚C for 15 min, 85˚C for 30 sec and 4˚C for 5 min. qPCR was performed using SYBR® Green master mix (Shanghai Yeasen Biotechnology Co., Ltd. and GAPDH was used as the internal reference. The primer sequences for target genes were as follows: AURKB forward, 5'-CAGTGGGACACCCGACATC-3' and reverse, 5'-GTACACGTTTCCAAACTTGCC-3'; BUB1 forward, 5'-TGGGAAAGATACATACAGTGGGT-3' and reverse, 5'-AGGGGATGACAGGGTTCCAAT-3'; BUB1B forward, 5'-AAATGACCCTCTGGATGTTTGG-3' and reverse, 5'-GCATAAACGCCCTAATTTAAGCC-3'; CCNB1 forward, 5'-AATAAGGCGAAGATCAACATGGC-3' and reverse, 5'-TTTGTTACCAATGTCCCCAAGAG-3'; CCNB2 forward, 5'-CCGACGGTGTCCAGTGATTT-3' and reverse, 5'-TGTTGTTTTGGTGGGTTGAACT-3'; CDC20 forward, 5'-GCACAGTTCGCGTTCGAGA-3' and reverse, 5'-CTGGATTTGCCAGGAGTTCGG-3'; CDCA8 forward, 5'-GAAGGGCAGTAGTCGGGTG-3' and reverse, 5'-TCACGGTCGAAGTCTTTCAGA-3'; CDK1 forward, 5'-AAACTACAGGTCAAGTGGTAGCC-3' and reverse, 5'-TCCTGCATAAGCACATCCTGA-3'; PLK1 forward, 5'-AAAGAGATCCCGGAGGTCCTA-3' and reverse, 5'-GGCTGCGGTGAATGGATATTTC-3'; RPS5 forward, 5'-ATGACCGAGTGGGAGACAG-3' and reverse, 5'-GCTTTGCGGAAGCGTTTGG-3'; RPS7 forward, 5'-GTGAAGCCCAATGGCGAGAA-3' and reverse, 5'-TGAGGTCCGAGTTCATCTCCA; RPS8 forward, 5'-TGAGGTCCGAGTTCATCTCCA-3' and reverse, 5'-AGCACGATGCAATTCTTCACC;-3' RPS14 forward, 5'-CCATGTCACTGATCTTTCTGGC-3' and reverse, 5'-TCATCTCGGTCTGCCTTTACC-3'; RPS27 forward, 5'-ATGCCTCTCGCAAAGGATCTC-3' and reverse, 5'-TGAAGTAGGAATTGGGGCTCT-3'; RPSA forward, 5'-GTGGCACCAATCTTGACTTCC-3' and reverse, 5'-GCAGGGTTTTCAATGGCAACAA-3'; TOP2A forward, 5'-ACCATTGCAGCCTGTAAATGA-3' and reverse, 5'-GGGCGGAGCAAAATATGTTCC-3'; GAPDH forward, 5'-GGAGCGAGATCCCTCCAAAAT-3' and reverse, 5'-GGCTGTTGTCATACTTCTCATGG-3'. The reaction was performed using the following thermocycling conditions: Initial denaturation at 95˚C for 30; 40 cycles of 95˚C for 30 sec and 60˚C for 30 sec. The relative level of gene expression was calculated using the $2^{-\Delta\Delta Cq}$ method (14).

Immunohistochemistry (IHC). The tissue samples were fixed in 4% paraformaldehyde for 24 h at room temperature, dehydrated using ethyl alcohol (98%) at 40˚C and embedded in paraffin (Wuhan Boster Biological Technology, Ltd.,) and subsequently cut into 4-μm sections. The samples were then deparaffinized using xylene and rehydrated at room temperature in a descending alcohol series. Following antigen retrieval with sodium citrate at 100˚C, the samples were treated with 3% hydrogen peroxide to block endogenous peroxidase activity, and then blocked with 5% BSA (Wuhan Boster Biological Technology, Ltd.,) for 30 min at room temperature. The specimens were subsequently incubated with a primary anti-RPS8 antibody (1:40; cat. no. 18228-1-AP; ProteinTech Group, Inc.,) for 12 h at 4˚C, followed by incubation with horseradish peroxidase (HRP)-conjugated secondary antibody (1:100; cat. no. G1210-2-A-100; Wuhan Servicebio Technology Co., Ltd.) for 2 h at room temperature. After development using the Cell and Tissue Staining HRP-DAB kit (Beyotime Institute of Biotechnology) according to the manufacturer's protocol, images were captured with an orthophoto light microscope (magnification, x200). Finally, the protein levels of RPS8 were evaluated according to the percentage scores. The proportion of positive cells were scored as follows: 0 (0-1%), 1 (1-33%), 2 (34-66%) and 3 (67-100%). The percentage scores were determined using Image-Pro Plus software (version 6.0; Media Cybernetics, Inc.). If the percentage scores in tumor tissues (alcohol- or non-alcohol-associated HCC) was higher compared with that in the corresponding adjacent tissues, the protein levels of RPS8 was determined to be upregulated.

Gene set enrichment analysis (GSEA). Good samples were divided into two groups (high and low) based on the median expression level of RPS8 [log (FPKM+1), 7.44]. To identify the potential pathways regulated by RPS8, GSEA software (version 4.0.0; Broad Institute Inc; http://software.broadinstitute.org/gsea/index.jsp) was used to determine whether a series of pathways were enriched in the gene rank derived from the differentially expressed genes between the two groups (high vs. low). Normalized enrichment score (NES) was used to predict the association between RPS8 and the enriched pathways; the higher the score indicates a stronger association). Terms with $P<0.01$ and NES >1.5 were used as the cut-off values.

Statistical analysis. The RT-qPCR experiment was repeated three times to detect the expression of target genes and the data are presented as the mean ± standard deviation. All statistical analyses in the present study were performed using SPSS v21.0 (IBM Corp). Comparisons between HCC tissues and adjacent normal tissues were performed using paired t-test. $P<0.05$ was used to indicate a statistically significant difference.

Results

Identification of good samples and good genes in alcohol-associated HCC from TCGA. The gene data profiles and clinical traits of 68 patients with alcohol-associated HCC were obtained from TCGA database. The results from using

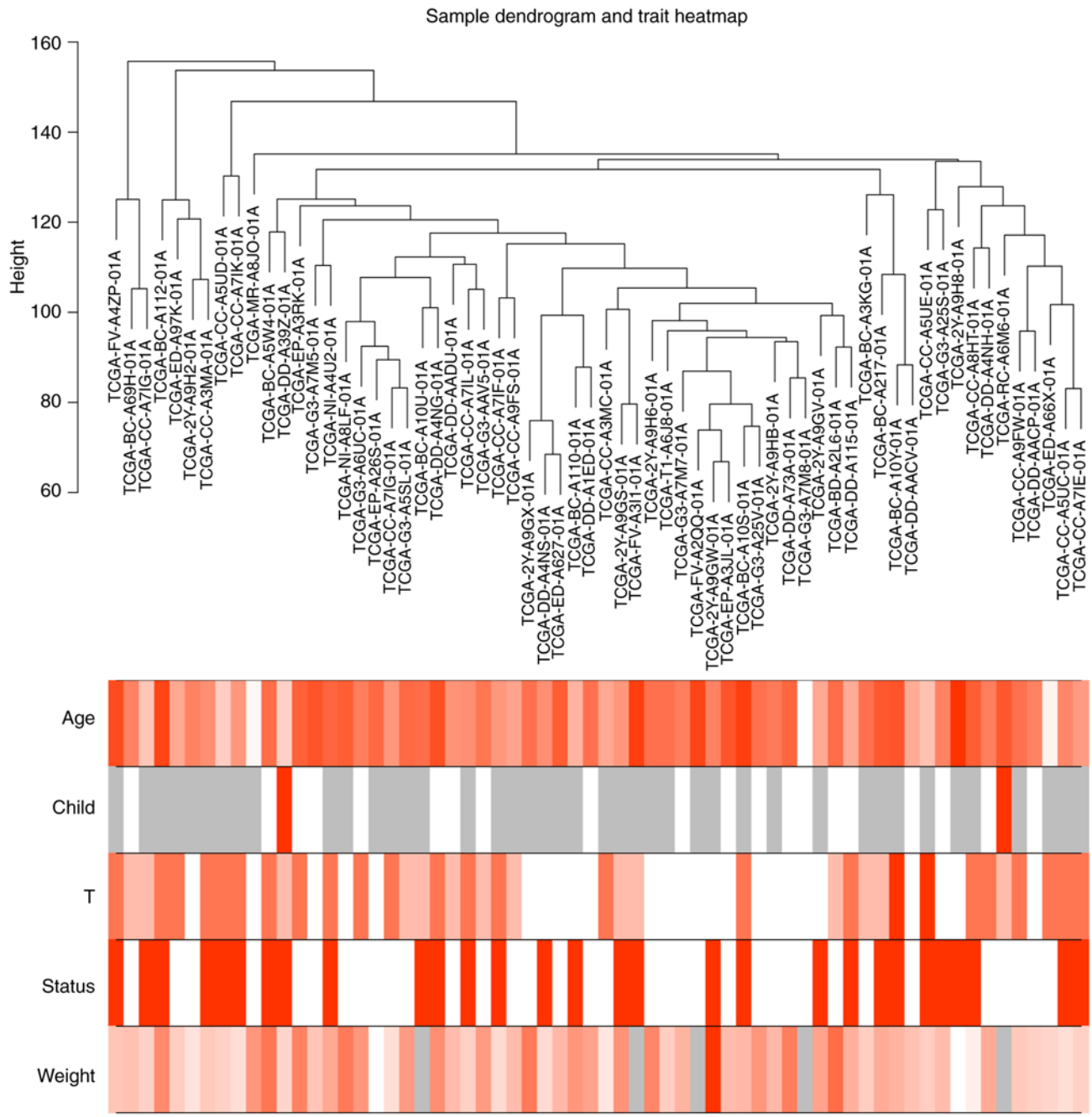

Figure 1. Sample tree clustering and clinical trait heat map of good samples. Following removal of outliers using the cut-off Height score >160, the remaining 64 alcohol-associated HCC profiles were analyzed and shown as a dendrogram, with their corresponding clinical traits (age, Child-Pugh score, TNM-T stage, status (dead or alive) and weight) as a heatmap. In the heatmap, the depth of the red color for age is proportional to time; the depth of the red color for Child-Pugh score are divided into 2 scales according to stage 1 and 2; the depth of the red color for TNM-T stage are divided into 4 scales according to stage 0-3; the depth of the red color for status are divided into 2 scales according to alive or dead; the depth of the red color for patient weight is proportional to the body mass index of the patient. The white color in each trait represents the lowest stage. The grey color indicates missing clinical trait information. HCC, hepatocellular carcinoma; TNM, tumor-node-metastasis.

the Hclust algorithm for gene expression profile revealed that 4 of the samples were outliers with a height score >160, which were excluded from subsequent analyses. The remaining 64 samples were identified as good samples and are shown in the sample dendrogram and clustered according to the height score of each sample; the corresponding clinical traits of these patients, including age, Child-Pugh score, T-stage, patient status (dead or alive) and body weight were also shown in the heatmap and used for further analysis (Fig. 1). Similarly, following removal of the probes without gene symbols, and genes with a mean expression level <0.5, the remaining 15,195 genes were determined to be good genes. Good genes and good samples were used to conduct WGCNA.

WGCNA to identify 'good samples' and 'good genes'. To ensure a high degree of independence (≥0.85; red line) (Fig. 2A) and low mean connectivity (~0.0) (Fig. 2B), a soft power of β=14 was used between the soft power of 1-20 (red

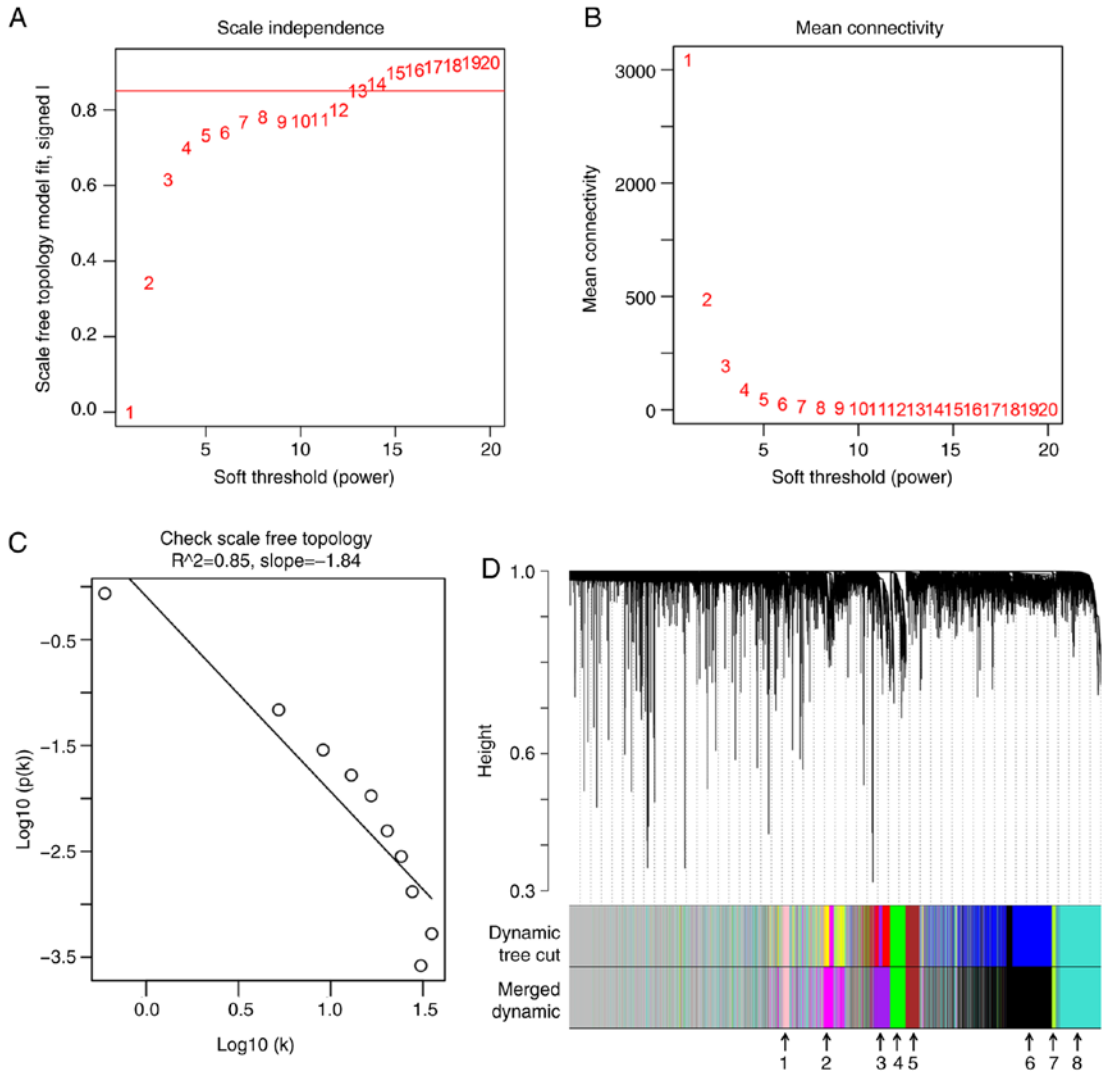

Figure 2. WGCNA for the gene expression profile of 64 alcohol-associated hepatocellular carcinoma from The Cancer Genome Atlas database. (A and B) Scale independence and mean connectivity of various soft-threshold values (β). The red number indicates the different soft threshold values (1-20), while the red lines indicates the cut-off values selected, as the scale independence >0.85. (C) Gene sets (black circles) with corresponding log10 (connectivity) and log10 P-value (connectivity) when the scale-free topology is set as β=14. (D) Clustering dendrograms of all genes with dissimilarity based on topological overlap, together with assigned module colors. Different colors represent different gene modules and there are 8 co-expressed modules (merged dynamic) in the WGCNA network and the 8 co-expressed modules were indicated using arrows (1, pink; 2, magenta; 3, purple; 4, green; 5, brown; 6, black, 7, green-yellow, and 8, turquoise). WGCNA, weighted gene co-expression network analysis.

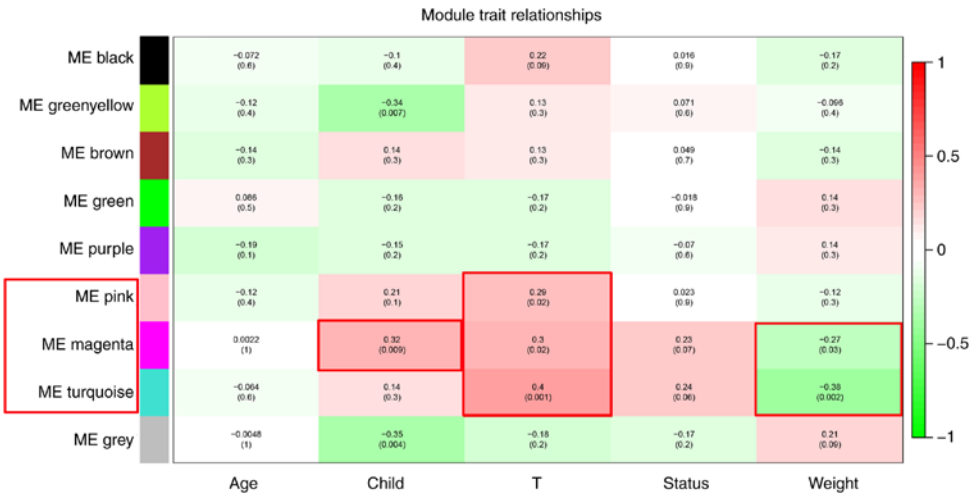

Figure 3. Identification of significant modules associated with clinical traits. Each cell in the heat map contains the corresponding correlation score and P-value. Red indicates positive correlation, while green indicates negative correlation. Gene modules positively associated clinical traits are highlighted.

Table I. GO analysis of core genes in the pink module following weighted gene co-expression network analysis.

Category	ID	Term	Count	P-value	Genes
BP	GO: 0046621	Negative regulation of organ growth	2	0.010954509	PTK2, STK3
BP	GO: 0000462	Maturation of SSU-rRNA from tricistronic rRNA transcript (SSU-rRNA, 5.8S rRNA, LSU-rRNA)	2	0.040116439	UTP23, DCAF13
CC	GO: 0032040	Small-subunit processome	2	0.042149642	UTP23, DCAF13

GO, Gene Ontology; BP, biological processes; CC, cellular components; SSU, small subunit; LSU, large subunit.

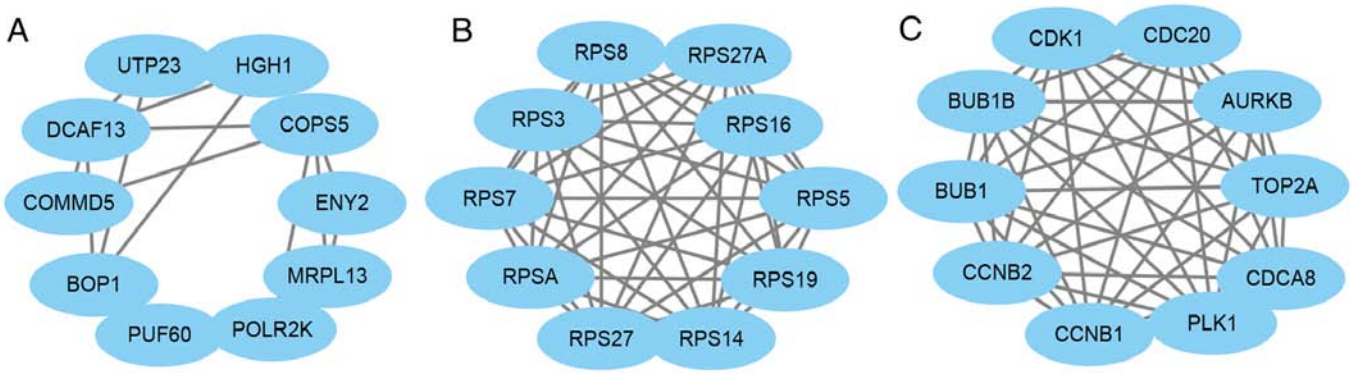

Figure 4. Protein-protein interaction network analysis of the hub genes within each gene module. (A) Pink module. (B) Magenta module. (C) Turquoise module. Grey lines in the network indicates the relationship between genes.

numbers). Furthermore, scale free topology also verified that β=14 could ensure independence >0.85 (Fig. 2C). The dissimilarity of the modules was set as 0.2, and a total of 8 co-expressed gene modules (black, green-yellow, brown, green, purple, pink, magenta and turquoise) were identified with a module size cut-off ≥100. The grey colored clusters represent the non-clustering genes (Fig. 2D).

Pink, magenta and turquoise modules were significant modules positively associated with the development of alcohol-associated HCC. The association between modules and clinical trait data was analyzed using WGCNA. The results revealed that 4 gene co-expressed modules were associated with clinical traits. The genes in the green-yellow module were negatively associated with Child-Pugh score (R=-0.34; P=0.007), while genes in the pink module were positively associated with T-stage (R=0.29; P=0.02). Genes in the magenta module were positively associated with Child-Pugh score (R=0.32; P=0.009) and T-stage (R=0.3; P=0.02) and negatively associated with the weight of the patient (R=-0.27; P=0.03). The turquoise module was positively associated with T-stage (R=0.4; P=0.001) and negatively associated with the weight of the patient (R=-0.38; P=0.002) (Fig. 3). Positive associations with Child-Pugh score and T-stage, and negative associations with the weight of the patient are all unfavorable traits for patients with alcohol-associated HCC and indicates the development of alcohol-associated HCC. Therefore, genes in the modules associated with unfavorable traits were further analyzed to identify hub genes positively associated with the development of alcohol-associated HCC and were considered to be oncogenes. In the pink, magenta and turquoise modules, 37, 111 and 204 genes with module membership >0.8 were identified as module core genes, respectively.

GO and KEGG analysis of module core genes. GO and KEGG analysis are methods used to identify the function and pathways the genes of interest are involved in (15). Therefore, the genes identified in the modules following WGCNA were subsequently analyzed to identify the pathways they are enriched in. The module core genes in the pink module were only enriched in the biological processes (BP) 'negative regulation of organ growth', 'maturation of SSU-rRNA from tricistronic rRNA transcript' and the cellular components (CC) 'small-subunit processome' (Table I). The top 10 terms in which the magenta module core genes were enriched for were 'protein binding' and 'poly(A) RNA binding' for molecular function (MF), 'cytosol', 'membrane', 'cytoplasm' and 'nucleus' for CC and 'rRNA processing', 'translational initiation', 'SRP-dependent cotranslational protein targeting to membrane' and 'viral transcription' for BP (Table II). The top 10 terms in which the turquoise module core genes were enriched for were 'cytoplasm', 'nucleoplasm', 'nucleus', 'membrane', 'nucleolus' and 'centrosome' for CC, and 'ATP binding', 'DNA binding', 'chromatin binding' and 'nuclear chromosome' for MF (Table III). The pink module core genes were not enriched in any pathway from KEGG analysis; however, the magenta module hub genes were enriched in the 'ribosome' and 'spliceosome' pathways (Table IV), while the turquoise module hub genes were

Table II. GO analysis of core genes in the magenta module following weighted gene co-expression network analysis.

Category	ID	Term	Count	P-value	Genes
MF	GO: 0005515	Protein binding	60	$1.02x10^{-4}$	CLTA, HRAS, RPL36A, PTGES2, RPL19, RPL14, SNRPD1, COPS9, RPLP2, SNRPD2, RPS3, RPLP1, LSM4, RPS27A, IMPDH2, PRPF31, RPL35A, EMG1, CCDC137, PA2G4, RPS19, RPS16, NME1, RPS14, PFDN5, UBE2M, MZT2B, RPS13, RPS10, RPS11, DYNLRB1, UBA52, SEC61G, RPL27A, NMB, ARPC4, RPS27, EIF3B, MYL6B, PSMB3, RPL9, GEMIN7, RPSA, LAMTOR4, RPS9, RPL23A, RPL24, ZNF524, RPS5, FBL, RPL28, RPS7, HSPBP1, NOSIP, RPL23, RPL18A, DPM2, RPL37A, POP7, TXNL4A
	GO: 0044822	Poly(A) RNA binding	47	$3.83x10^{-33}$	RPL36A, RPL19, RPL14, RPL27A, RPL35, SNRPD1, RPL36, SNRPD2, RPS3, RPS27, RPL32, REXO4, CCDC124, LSM4, RPS21, RPS27A, RPSA, RPL35A, PRPF31, RRP1, EMG1, RPL27, RPS9, RPL24, RPL23A, CCDC137, RRP9, RPS5, RPL28, FBL, RPS8, RPL29, RPS7, PA2G4, NOSIP, RPS19, RPS16, RPL18A, RPL23, RPL13A, NME1, RPS14, RPS13, RPL37A, RPS10, RPS11, POP7
CC	GO: 0005829	Cytosol	58	$2.34x10^{-24}$	RPL18, CLTA, HRAS, RPL36A, PTGES2, RPL19, RPL14, SNRPD1, RPLP2, SNRPD2, RPS3, RPLP1, LSM4, RPS27A, IMPDH2, NT5C, RPL35A, RPS19, RPS16, NME1, RPS14, UBE2M, RPS13, RPS10, RPS11, UBA52, SEC61G, POLR2H, RPL35, RPL27A, RPL36, RPL37, ARPC4, RPL38, RPS27, EIF3B, RPL32, MYL6B, PSMB3, RPL9, RPS21, GEMIN7, RPSA, RPS9, RPL27, RPL23A, RPL24, RPS5, RPS8, RPL28, RPS7, RPL29, ITPA, NOSIP, RPL23, RPL18A, RPL13A, RPL37A
	GO: 0016020	Membrane	41	$2.77x10^{-16}$	RPL18, CLTA, HRAS, RPL19, RPL14, RPL27A, RPL35, RPLP2, RPL36, RPS3, RPL32, RPL9, IMPDH2, RPS27A, PTDSS2, RPSA, RPL35A, RPL27, RPS9, RPL24, BCL2L12, RPS5, RPL28, FBL, RPS8, RPL29, RPS7, PA2G4, RPS19, RPS16, RPL18A, RPL23, CD320, NME1, RPL13A, RPS14, RPS13, RPS10, RPS11, DYNLRB1, SEC61G
	GO: 0005737	Cytoplasm	41	$8.96x10^{-5}$	RPL18, HRAS, RPL19, RPL14, RPL35, COPS9, RPL36, RFXANK, RPS3, EIF3B, CCDC124, PSMB3, RPL9, RPLP1, RPS21, GEMIN7, RPS27A, IMPDH2, NT5C, RPSA, EMG1, RPS9, RPL24, RPL23A, RPL28, RPS8, RPS7, PA2G4, NOSIP, ITPA, RPS19, RPL23, RPL13A, NME1, PFDN5, RPS14, UBE2M, RPS11, DYNLRB1, POP7, TXNL4A
	GO: 0005634	Nucleus	40	$4.85x10^{-4}$	RPL18, POLR2H, HRAS, PTGES2, SNRPD1, COPS9, RFXANK, RPS3, RPS27, REXO4, PSMB3, RPL9, GEMIN7, RPS27A, IMPDH2, NT5C, RPSA, PRPF31, RRP1, EMG1, RPL27, RPS9, RPL23A, RRP9, BCL2L12, ZNF524, FBL, RPS8, RPS7, PA2G4, NOSIP, RPL13A, NME1, PFDN5, RPS13, SURF2, RPL37A, UBA52, POP7, TXNL4A

Table II Continued.

Category	ID	Term	Count	P-value	Genes
BP	GO: 0006364	rRNA processing	44	$1.06x10^{-61}$	RPL18, RPL36A, RPL19, RPL14, RPL27A, RPL35, RPLP2, RPL36, RPL37, RPL38, RPS3, RPS27, RPL32, RPL9, RPLP1, RPS21, RPS27A, RPSA, RPL35A, RRP1, EMG1, RPL27, RPS9, RPL24, RPL23A, RRP9, RPS5, RPL28, FBL, RPS8, RPL29, RPS7, PA2G4, RPS19, RPS16, RPL18A, RPL23, RPL13A, RPS14, RPS13, RPS10, RPL37A, RPS11, UBA52
	GO: 0006413	Translational initiation	40	$3.93x10^{-62}$	RPL18, RPL36A, RPL19, RPL14, RPL27A, RPL35, RPLP2, RPL36, RPL37, RPL38, RPS3, RPS27, EIF3B, RPL32, RPL9, RPLP1, RPS21, RPS27A, RPSA, RPL35A, RPL27, RPS9, RPL24, RPL23A, RPS5, RPL28, RPS8, RPL29, RPS7, RPS19, RPS16, RPL18A, RPL23, RPL13A, RPS14, RPS13, RPS10, RPL37A, RPS11, UBA52
	GO: 0006614	SRP-dependent cotranslational protein targeting to membrane	39	$1.99x10^{-67}$	RPL18, RPL36A, RPL19, RPL14, RPL27A, RPL35, RPLP2, RPL36, RPL37, RPL38, RPS3, RPS27, RPL32, RPL9, RPLP1, RPS21, RPS27A, RPSA, RPL35A, RPL27, RPS9, RPL24, RPL23A, RPS5, RPL28, RPS8, RPL29, RPS7, RPS19, RPS16, RPL18A, RPL23, RPL13A, RPS14, RPS13, RPS10, RPL37A, RPS11, UBA52
	GO: 0019083	Viral transcription	39	$7.41x10^{-64}$	RPL18, RPL36A, RPL19, RPL14, RPL27A, RPL35, RPLP2, RPL36, RPL37, RPL38, RPS3, RPS27, RPL32, RPL9, RPLP1, RPS21, RPS27A, RPSA, RPL35A, RPL27, RPS9, RPL24, RPL23A, RPS5, RPL28, RPS8, RPL29, RPS7, RPS19, RPS16, RPL18A, RPL23, RPL13A, RPS14, RPS13, RPS10, RPL37A, RPS11, UBA52

GO, Gene Ontology; BP, biological processes; CC, cellular components; MF molecular function.

Table III. GO analysis of core genes in the turquoise module following weighted gene co-expression network analysis.

Category	ID	Term	P-value	Genes
CC	GO: 0005737	Cytoplasm	2.78×10^{-6}	RAD51D, PRC1, EZH2, PRR11, PKMYT1, PTTG1, MCM10, FANCI, CDCA2, ORC1, CDCA5, CDK1, MCRS1, KIF11, STK25, DSN1, DTL, MTA3, NUSAP1, MCM2, TACC3, UBE2C, ECT2, RAD51, NCAPD2, CAPN10, SGO1, FANCD2, ZWINT, STMN1, MELK, UBE2T, NEK2, FOXM1, POLA1, COPS7B, NDC1, SRRT, NCAPG, HJURP, SPATS2, BUB1, ERCC6L, GIT1, EXO1, DLGAP5, EME1, KIF18A, CDC20, BIRC5, SPDL1, ZBED8, RACGAP1, CENPI, BRCA1, PLK1, POLD1
	GO: 0005654	Nucleoplasm	6.24×10^{-18}	KIF23, ITGB3BP, RAD51D, PRC1, AURKB, FANCI, CDCA2, NUP37, CDCA5, TOP2A, KHDRBS1, CDC6, DTL, LIG1, RBL1, TPX2, MCM2, MCM3, MCM4, MCM5, HNRNPU, MCM6, RAD51, NCAPD2, RAD1, SGO2, SGO1, RAD18, THOC5, KPNA2, LMNB1, FOXM1, TIPIN, POLA1, ANLN, CHEK1, MYBL2, HNRNPA3, HNRNPL, SRRT, BUB1, WDHD1, FEN1, ERCC6L, CENPO, EXO1, NASP, CDC20, ZBED8, RACGAP1, RAD54L, POLD1, TUBD1, RBM14, CHAF1B, PIP4K2B
	GO: 0005634	Nucleus	6.98×10^{-5}	RALY, DTYMK, PRR11, PKMYT1, PTTG1, CDT1, TLK2, CDCA5, TOP2A, CDCA4, LIG1, RBL1, CCNF, MCM2, UBE2C, ECT2, HNRNPU, RAD51, ZSWIM1, SGO1, FANCD2, RRM2, RAD18, MELK, UBE2T, NEK2, FOXM1, CERS5, MYBL2, VPS72, HJURP, CENPA, RHNO1, ASF1B, TPRKB, DLGAP5, KIF18A, NUF2, SPDL1, BIRC5, EHMT2, BRCA1, CENPI, SUV39H2, CENPH, CCNB1, CCNB2, WDR62, SFPQ, CHAF1B
	GO: 0016020	Membrane	5.67×10^{-9}	KIFC1, PRR11, PKMYT1, TTK, COIL, HNRNPL, KIF2C, NCAPH, FANCI, NCAPG, EDC3, BUB1, GIT1, KHDRBS1, CDK1, KIF11, MKI67, MSH2, KIF15, NUF2, NUP85, NDC80, NUP155, MCM3, MCM4, RBMX, MCM5, HNRNPU, NCAPD2, POLD1, STMN1, KPNA2, NKIRAS2
	GO: 0005730	Nucleolus	3.09×10^{-4}	MCRS1, MKI67, DTL, POLA1, NUSAP1, MCM10, PPP1CC, COIL, RAD51, CDCA8, FANCD2, HJURP, PLK1, RAE1, FANCG, ORC1, TOP2A, FEN1
	GO: 0005813	Centrosome	9.07×10^{-7}	RAD51D, KIF23, CDK1, HAUS5, XRCC2, NEK2, DTL, CHEK1, MCM3, CDC45, SGO1, WDR62, NCAPG, PLK1, CKAP2L, RAD18, ERCC6L
MF	GO: 0005524	ATP binding	1.09×10^{-13}	KIF23, RAD51D, KIFC1, KIF4A, XRCC2, NEK2, DTYMK, PKMYT1, TTK, CHEK1, AURKB, KIF2C, BUB1, TLK2, CDK16, TOP2A, ORC1, ERCC6L, TRIP13, CDK1, CDC6, KIF11, STK25, MSH2, LIG1, KIF15, KIF18A, KIF18B, ATAD5, CENPE, MCM2, MCM3, UBE2C, MCM4, RAD54L, MCM5, MCM6, RAD51, RFC4, PLK1, MYO19, UBE2T, MELK, KIF20A
	GO: 0003677	DNA binding	1.00×10^{-4}	EXO1, LIG1, EME1, TIPIN, POLA1, CERS5, MCM2, ZBED8, MCM3, BRCA1, CDT1, SRRT, POLD1, PRIM2, H2AFZ, CENPW, FEN1
	GO: 0003682	Chromatin binding	6.55×10^{-7}	EXO1, CDK1, CDC45, POLD1, MTA3, POLA1, FAAP24, ACTL6A, CDCA5, RBMX, TOP2A, ORC1, UBE2T, MCM5, NCAPD2, RAD51

GO, Gene Ontology; CC, cellular components; MF molecular function.

Table IV. Kyoto Encyclopedia of Genes and Genomes analysis of core genes in the magenta module following weighted gene co-expression network analysis.

ID	Term	Count	P-value	Genes
hsa03010	Ribosome	39	6.2923×10^{-50}	RPL18, RPL36A, RPL19, RPL14, RPL27A, RPL35, RPLP2, RPL36, RPL37, RPL38, RPS3, RPS27, RPL32, RPL9, RPLP1, RPS21, RPS27A, RPSA, RPL35A, RPL27, RPS9, RPL24, RPL23A, RPS5, RPL28, RPS8, RPL29, RPS7, RPS19, RPS16, RPL18A, RPL23, RPL13A, RPS14, RPS13, RPS10, RPL37A, RPS11, UBA52
hsa03040	Spliceosome	5	0.036532189	PRPF31, SNRPD1, LSM4, SNRPD2, TXNL4A

Table V. Kyoto Encyclopedia of Genes and Genomes analysis of module core genes in the turquoise module following weighted gene co-expression network analysis.

ID	Term	Count	P-value	Genes
Hsa04110	Cell cycle	23	6.88×10^{-21}	E2F1, E2F2, CDC6, CDK1, RBL1, PKMYT1, TTK, CHEK1, CDC20, PTTG1, MCM2, MCM3, MCM4, MCM5, MCM6, CCNB1, CDC45, CCNB2, PLK1, BUB1, BUB1B, ANAPC7, ORC1
hsa03030	DNA replication	11	5.06×10^{-12}	RFC4, LIG1, POLD1, PRIM2, POLA1, MCM2, MCM3, MCM4, MCM5, FEN1, MCM6
hsa04114	Oocyte meiosis	11	5.09×10^{-7}	CCNB1, CDK1, CCNB2, PLK1, SGO1, BUB1, PKMYT1, CDC20, PTTG1, ANAPC7, PPP1CC
hsa03460	Fanconi anemia pathway	8	2.21×10^{-6}	FANCD2, FANCI, EME1, FAAP24, FANCG, BRCA1, UBE2T, RAD51
hsa03440	Homologous recombination	6	1.79×10^{-5}	RAD51D, XRCC2, POLD1, EME1, RAD54L, RAD51
hsa03430	Mismatch repair	5	1.27×10^{-4}	EXO1, RFC4, MSH2, LIG1, POLD1
hsa04914	Progesterone-mediated oocyte maturation	7	4.89×10^{-4}	CCNB1, CDK1, CCNB2, PLK1, BUB1, PKMYT1, ANAPC7
hsa0411	5:p53 signaling pathway	6	1.03×10^{-3}	CCNB1, CDK1, CCNB2, RRM2, CHEK1, GTSE1
hsa03013	RNA transport	8	3.70×10^{-3}	NDC1, SUMO2, RAE1, NUP37, NUP85, THOC5, NUP155, TACC3
hsa05166	HTLV-I infection	9	9.02×10^{-3}	E2F1, DVL3, E2F2, POLD1, BUB1B, CHEK1, CDC20, PTTG1, ANAPC7
hsa00240	Pyrimidine metabolism	5	2.96×10^{-2}	POLD1, RRM2, DTYMK, PRIM2, POLA1

enriched in 'cell cycle', 'DNA replication', 'oocyte meiosis', 'fanconi anemia pathway', 'homologous recombination', 'mismatch repair', 'progesterone-mediated oocyte maturation', 'p53 signaling pathway', 'RNA transport', 'HTLV-I infection' and 'pyrimidine metabolism' (Table V).

PPI network construction of core genes. The core genes in the pink, magenta and turquoise modules were then used to construct a PPI network using STRING, while Cytoscape was used to analyze and determine the hub genes based on degree score. The results revealed that MRPL13, UTP23, HGH1, DCAF13, BOP1, PUF60, COMMD5, POLR2K, ENY2 and COPS5 were all hub genes in the pink module (Fig. 4A), while RPS19, RPS7, RPS5, RPS16, RPS3, RPS8, RPSA, RPS27A, RPS27 and RPS14 were hub gens in the magenta module (Fig. 4B). Furthermore, CDCA8, CDC20, BUB1B, AURKB, TOP2A, CDK1, CCNB1, PLK1, BUB1 and CCNB2 were hub genes in the turquoise module (Fig. 4C).

Progression and survival analysis of hub genes. Pearson's correlation analysis was performed to determine the association between hub gene expression and the progression of alcohol-associated HCC. The results indicated that the expression of AURKB, BUB1, BUB1B, CCNB1, CCNB2, CDC20, CDCA8, CDK1, PLK1, RPS5, RPS7, RPS8, RPS14, RPS27, RPSA and TOP2A was positively associated with the progression of alcohol-associated HCC ($P<0.01$; Fig. 5). Similarly, high expression levels of these genes were significantly associated with poor prognosis ($P<0.05$; Fig. 6). Taken together, these results indicate that AURKB, BUB1, BUB1B, CCNB1,

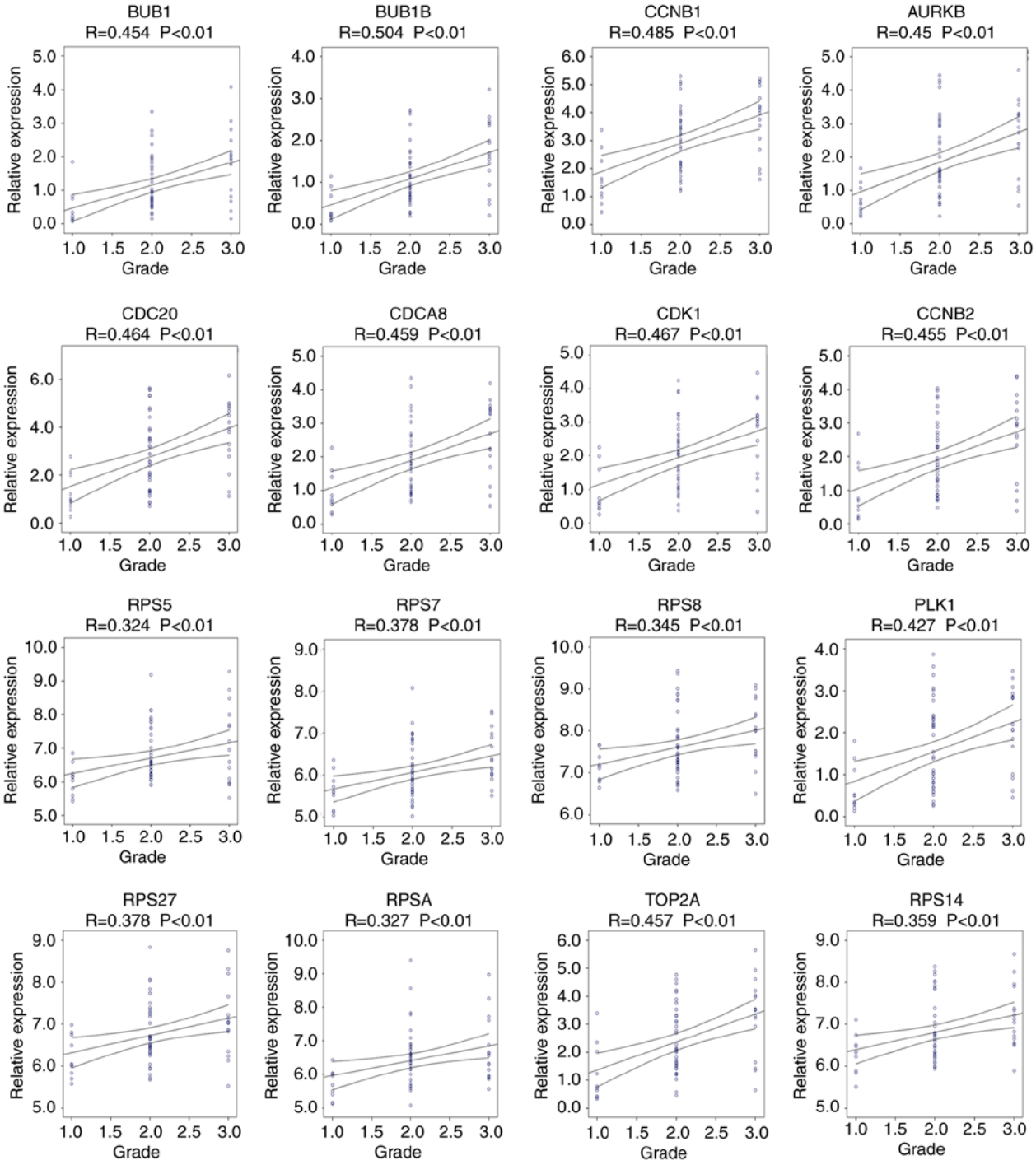

Figure 5. Pearson's correlation analysis to detect the effects of hub gene expression on the progression of alcohol-associated hepatocellular carcinoma. Grade, tumor grade.

CCNB2, CDC20, CDCA8, CDK1, PLK1, RPS5, RPS7, RPS8, RPS14, RPS27, RPSA and TOP2A may be real hub genes for alcohol-associated HCC.

RPS8 was specifically highly expressed in alcohol-associated HCC tissues. To determine whether the real hub genes identified in the present study were specific to alcohol-associated HCC, their mRNA and protein expression levels were verified in patients with non-alcohol- and alcohol-associated HCC. The RT-qPCR results revealed that the mRNA expression levels of AURKB, BUB1, BUB1B, CCNB1, CCNB2, CDC20, CDCA8, CDK1, PLK1, RPS7, RPS8, RPS14, RPS27, RPSA and TOP2A were significantly higher in patients with alcohol-associated HCC, but there was no significant difference for RPS5 (Fig. 7). The mRNA expression levels of the aforementioned genes were also significantly higher in non-alcohol-associated HCC; however, there was no significant difference with RPS8 and RPS5 (Fig. 8). As the mRNA expression level of RPS8 was found to be specifically highly expressed in alcohol-associated HCC tissues rather than in non-alcohol-associated HCC tissues from the RT-qPCR results, IHC was performed to further determine the protein

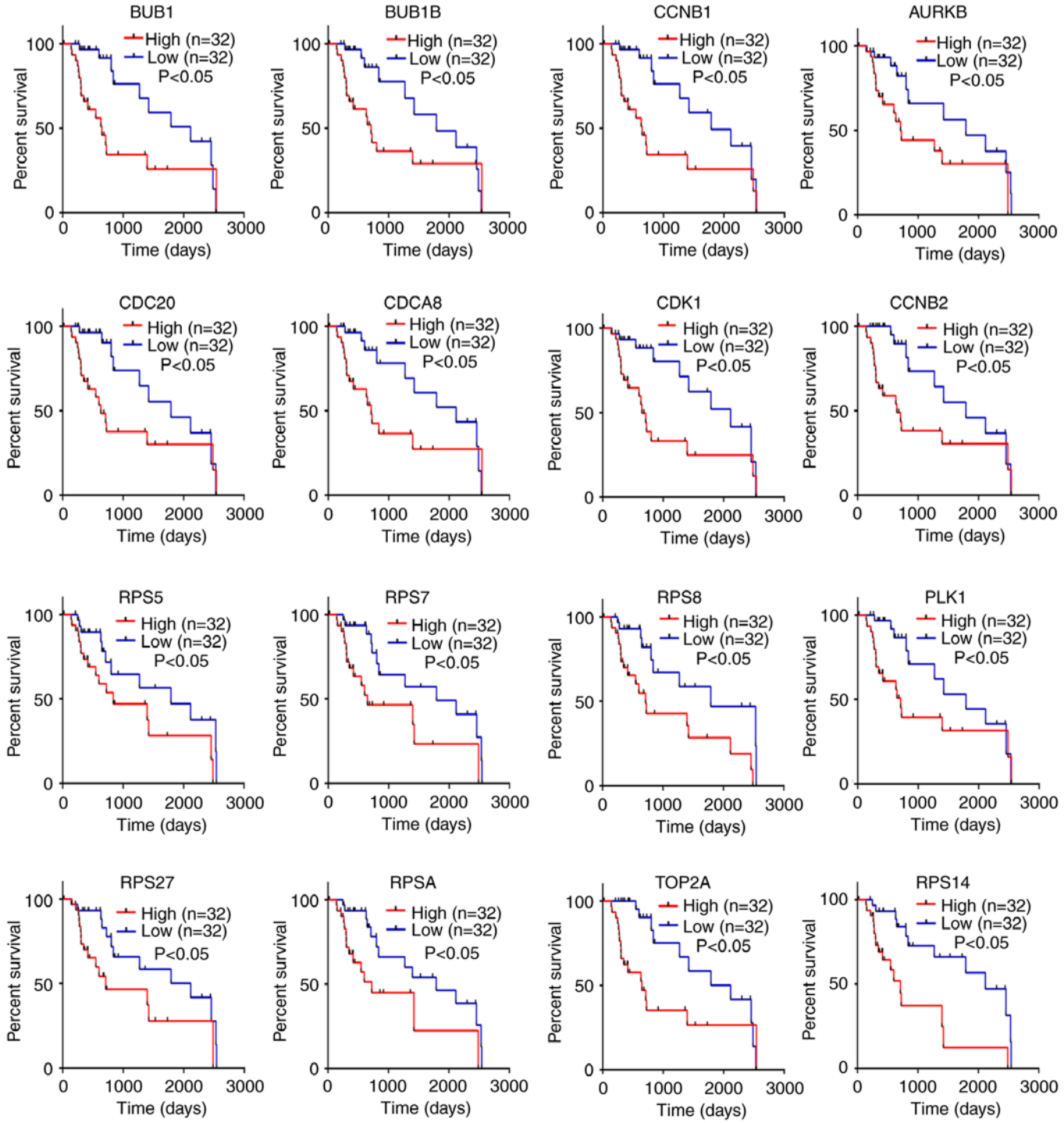

Figure 6. Kaplan-Meier survival analysis to detect the effects of hub gene expression on the overall survival times of patients with alcohol-associated hepatocellular carcinoma.

expression level of RPS8 in the tissues of patients with alcohol- and non-alcohol-associated HCC. The results revealed that the protein expression level of RPS8 was increased in 27 of the 30 alcohol-associated HCC tissues compared with that in their paired adjacent normal tissues; however, RPS8 was not increased in the non-alcohol-associated HCC tissues (Fig. 9). Taken together, these results indicate that AURKB, BUB1, BUB1B, CCNB1, CCNB2, CDC20, CDCA8, CDK1, PLK1, RPS7, RPS14, RPS27, RPSA and TOP2A may be common biomarkers for alcohol- and non-alcohol-associated HCC, while RPS8 may be specific biomarker for alcohol-associated HCC.

GSEA of RPS8 in TCGA. GSEA was performed to identify the pathways enriched in samples with high mRNA levels of RPS8. A total of 10 pathways were obtained, including 'RNA polymerase', 'ribosome', 'degradation', 'Huntington's disease', 'spliceosome', 'pyrimidine metabolism', 'purine metabolism', 'cell cycle', 'homologous recombination' and 'DNA replication' (Fig. 10). The results indicate that RPS8 may regulate

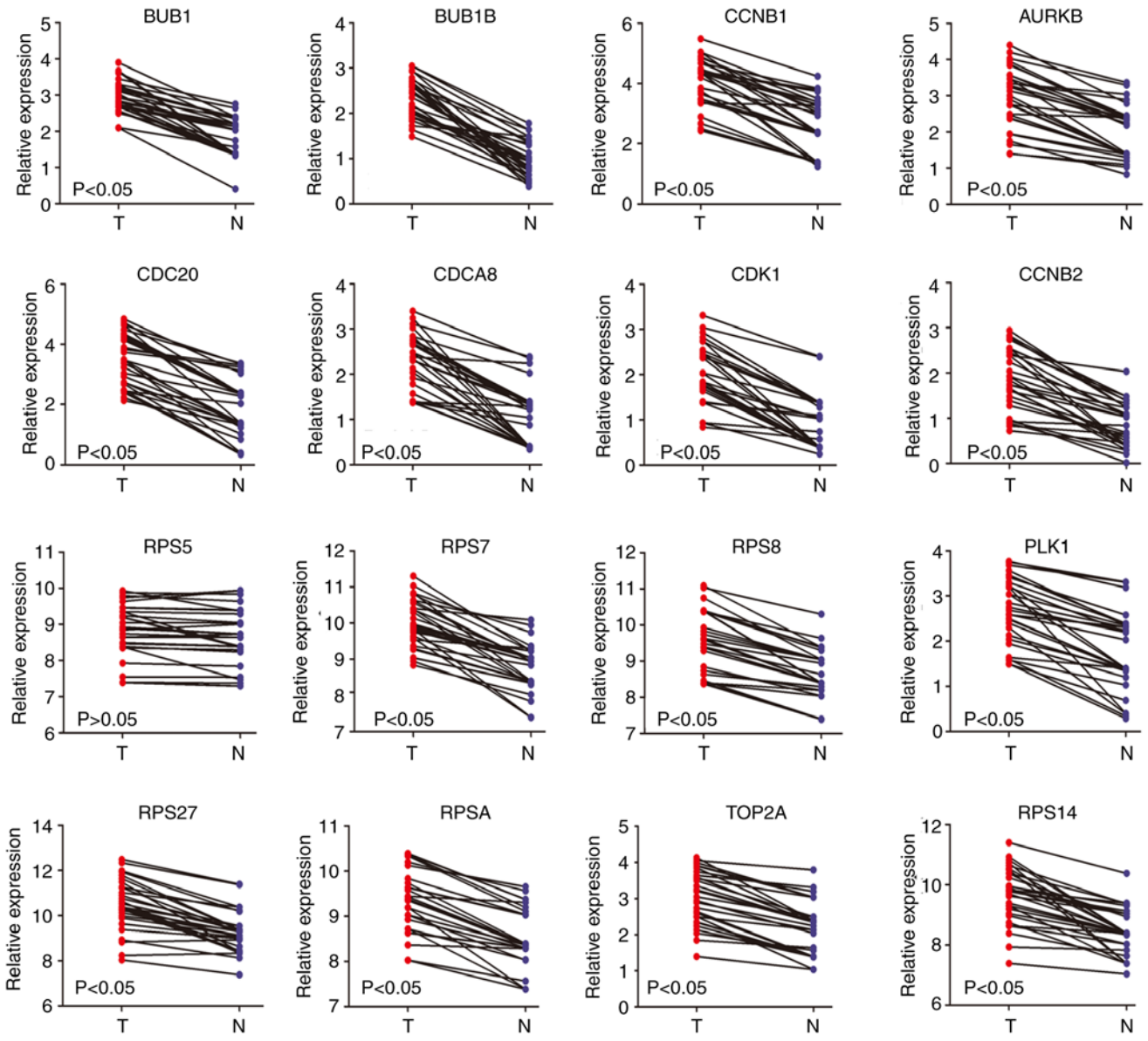

Figure 7. Reverse transcription-quantitative PCR detection of the expression levels of hub genes in alcohol-associated hepatocellular carcinoma tissues and corresponding adjacent normal tumor tissues. T, tumor; N, normal.

the progression of alcohol-associated HCC by affecting these pathways.

Discussion

Previous studies have demonstrated that the prognosis of patients with alcohol-associated HCC is lower compared with that of those with non-alcohol associated HCC (16,17). Furthermore, the risk of distant metastases and worse liver function is increased in patients with alcohol-associated HCC (18). Similarly, alcohol-associated HCC is harder to diagnose, and patients are commonly diagnosed at a late disease stage (16). A study, which enrolled 32,913 patients in 2019, demonstrated that the overall survival rate following liver transplant for alcohol-associated HCC was shorter compared with that for non-alcohol associated HCC (mean rate, 3.9 vs. 4.7) in USA (19). Therefore, the identification of key genes associated with alcohol-associated HCC may improve diagnosis and treatment.

In the present study, the gene expression profiles of patients with alcohol-associated HCC and their corresponding clinical traits, were downloaded from TCGA and used to perform WGCNA; 8 co-expressed genes were identified and 3 co-expressed gene modules were positively associated with the clinical traits. Following GO and KEGG analysis, and the construction of a PPI network, 30 hub genes were identified; 16 of which were associated with the progression of alcohol-associated HCC and were able to predict poor patient outcome. Among these 16 genes, only the mRNA expression level of RPS8 was significantly higher in alcohol-associated HCC, but not in non-alcohol-associated HCC, and there was no significant difference with RPS5 in both non-alcohol- and alcohol-associated HCC; the remaining 14 real hub genes, including AURKB, BUB1, BUB1B, CCNB1, CCNB2, CDC20, CDCA8, CDK1, PLK1, RPS7, RPS14, RPS27, RPSA and TOP2A, were highly expressed in both alcohol- and non-alcohol-associated HCC. It was therefore

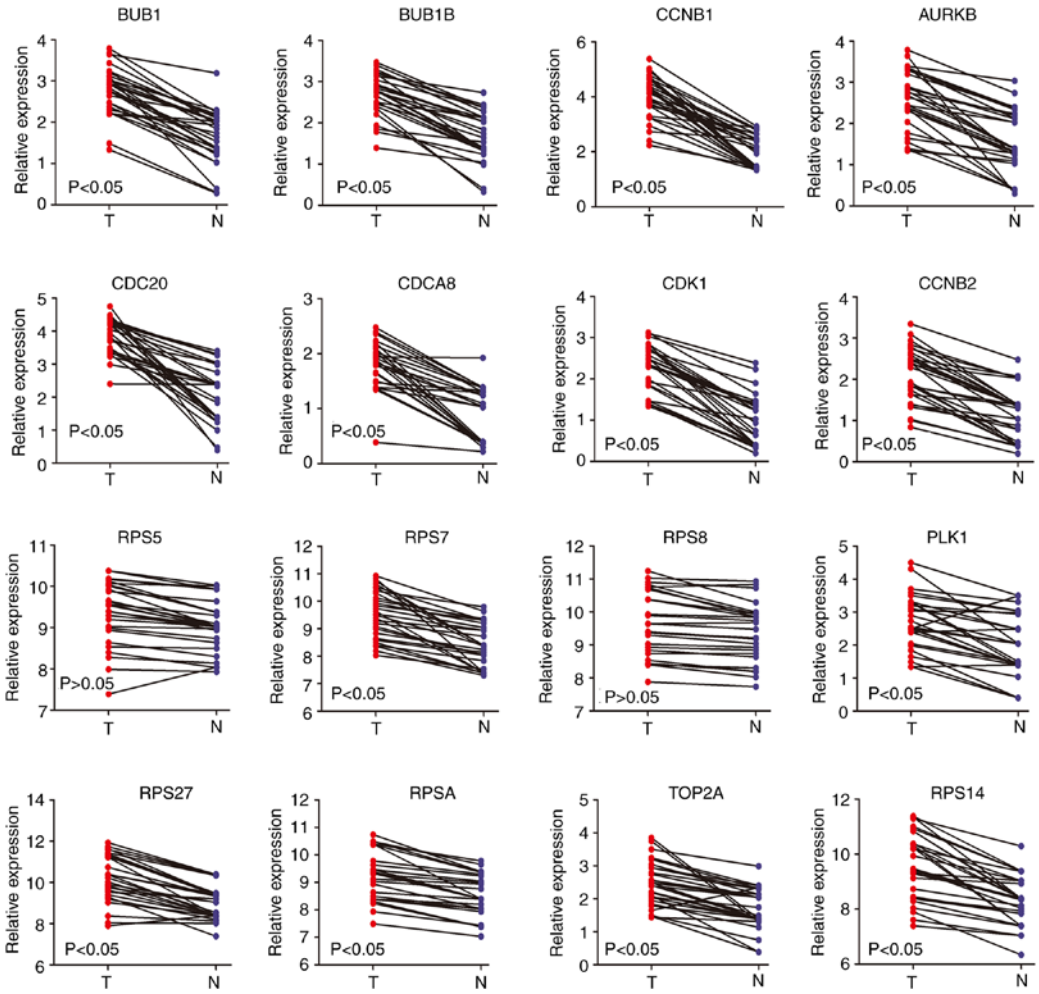

Figure 8. Reverse transcription-quantitative PCR detection of the expression levels of hub genes in non-alcohol-associated hepatocellular carcinoma tissues and corresponding adjacent normal tissues. T, tumor; N, normal.

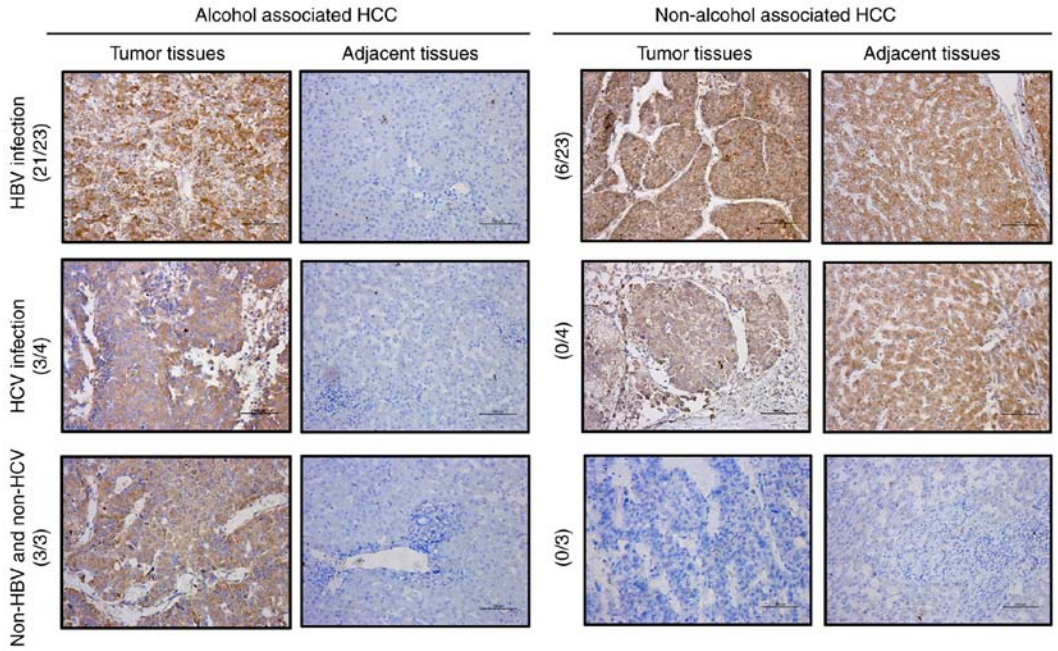

Figure 9. Immunohistochemical staining of tissues from patients with alcohol- and non-alcohol-associated hepatocellular carcinoma, and their corresponding adjacent normal tissues, to determine the expression of RPS8. The proportion of upregulation of RPS8 (HCC vs. adjacent normal tissues) in alcohol- and non-alcohol-associated HCC divided according to infection status (HBV, HCV or not infected). RPS8, 40S ribosomal protein S8; HCC, hepatocellular carcinoma; HBV, Hepatitis B Virus; HCV, hepatitis C virus.

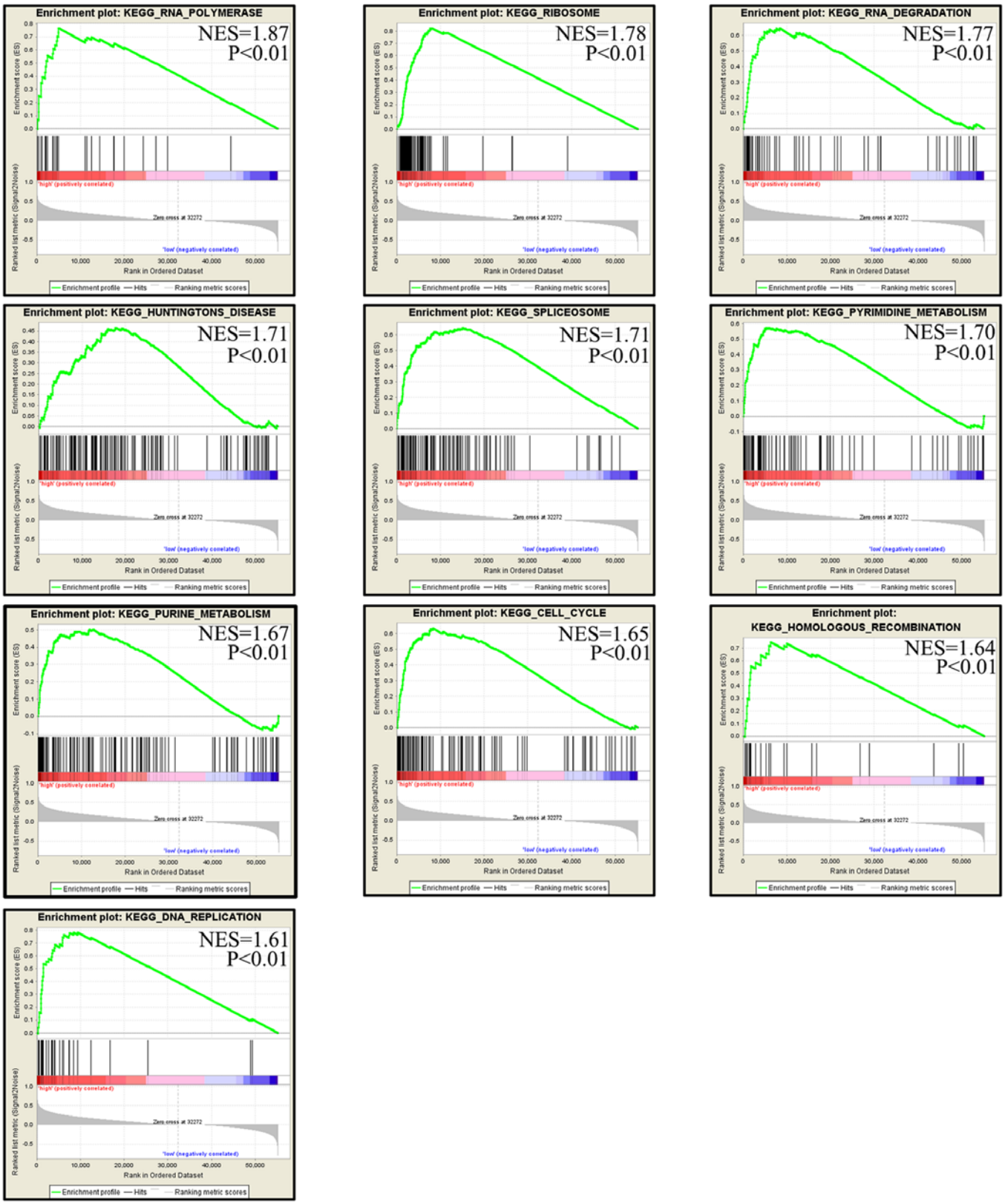

Figure 10. Gene set enrichment analysis of RPS8 in TCGA database. Enriched pathways with high expression levels of RPS8 (NES >1.5 and P<0.01). HCC, hepatocellular carcinoma; TCGA, The Cancer Genome Atlas; KEGG, Kyoto Encyclopedia of Genes and Genomes; NES, normalized enrichment score.

hypothesized that RPS8 may be a novel and specific biomarker for alcohol-associated HCC, while the remaining 14 real hub genes may be common biomarkers for both alcohol- and non-alcohol associated HCC.

The small ribosomal family proteins are important structural components of the ribosome, which serves a key role in protein synthesis (20). The functional biology and related molecular mechanisms of small ribosomal proteins have been

widely investigated (21). The mRNA expression level of RPS7 was found to be highly expressed in prostate cancer compared with that in adjacent normal tissues, and a high mRNA expression level of was also found to be positively associated with poor outcome via promoting cell proliferation (22). RPSA was revealed to activate AKT-related pathways and to promote pancreatic cancer cell metastasis (23). RPS5 was identified as a risk factor for recurrence and progression in patients with Dukes' B colon cancer (24). The small ribosomal protein family is also involved in HCC. RPS3 has been shown to post-transcriptionally upregulate the NAD-dependent protein deacetylase sirtuin-1 which promotes hepatocarcinogenesis (25). RPS6 promotes HCC cell proliferation and migration, which is regulated by the AKT/mTOR pathway (26). RPS8 is primarily located in cytoplasmic messenger ribonucleoprotein granules containing untranslated mRNAs, and is expressed in all organs and tissues in humans, and has no tissue specificity (27). In addition, previous studies have revealed that the mRNA expression level of RPS8 was increased in pancreatic cancer tissues and associated with poor outcome (28,29) and may promote gemcitabine resistance (30).

Previous studies have revealed that alcohol intake can alter the metabolic capacity of the liver (31). However, knowledge of its influence on biological function for all sub-types of HCC is limited. In the present study, GESA revealed that two metabolic pathways were enriched in samples with high mRNA expression levels of RPS8, including the 'pyrimidine-' and 'purine metabolism' pathways. Therefore, RPS8 is hypothesized to play a key role in alcohol-associated HCC by regulating these pathways. However, the exact role of RPS8 in alcohol-associated HCC requires further investigation. Moreover, the results of the present study require further validation with an increased sample population and relevant experimental investigation.

In conclusion, using WGCNA and additional analytical methods (GO, KEGG, PPI network, survival analysis, and GSEA), and RT-qPCR using patient samples, the results of the present study indicate that RPS8 may be a novel and specific biomarker for alcohol-associated HCC.

Acknowledgements

Not applicable

Funding

The present study was funded by grants from The National Natural Science Foundation of China (grant nos. 81560477, 81860505, 81860506 and 81660483), and Science and Technology Co-operation in Guizhou (grant nos. 5404, 09, and 5647).

Availability of data and materials

The datasets used and/or analyzed during the current study are available from the corresponding author on reasonable request.

Authors' contributions

NB, SL and YS performed the experiments. NB, YS, ZZ and YZ collected data, performed data analysis, and interpretation. CY, SL and CS designed the experiments and wrote the manuscript. All authors revised the manuscript and read and approved the final version of the article.

Ethics approval and consent to participate

The present study was approved by the Ethics Committee of Guizhou Medical University and performed in accordance with the Declaration of Helsinki. Informed consent was provided from all the patients.

Patient consent for publication

Not applicable.

Competing interests

The authors declare that they have no competing interests.

References

1. Bray F, Ferlay J, Soerjomataram I, Siegel RL, Torre LA and Jemal A: Global cancer statistics 2018: GLOBOCAN estimates of incidence and mortality worldwide for 36 cancers in 185 countries. CA Cancer J Clin 68: 394-424, 2018.
2. Li L, Li B and Zhang M: HBV DNA levels impact the prognosis of hepatocellular carcinoma patients with microvascular invasion. Medicine (Baltimore) 98: e16308, 2019.
3. Zhao H, Zhu P, Han T, Ye Q, Xu C, Wu L, Liu F, Yin W, Li Z and Guo Y: Clinical characteristics analysis of 1180 patients with hepatocellular carcinoma secondary to hepatitis B, hepatitis C and alcoholic liver disease. J Clin Lab Anal 34: e23075, 2019.
4. Tian L, Cervenka ND, Low AM, Olson DG and Lynd LR: A mutation in the AdhE alcohol dehydrogenase of Clostridium thermocellum increases tolerance to several primary alcohols, including isobutanol, n-butanol and ethanol. Sci Rep 9: 1736, 2019.
5. Garcia CC, Batista GL, Freitas FP, Lopes FS, Sanchez AB, Gutz IG, Di Mascio P and Medeiros MH: Quantification of DNA adducts in lungs, liver and brain of rats exposed to acetaldehyde. Free Radic Biol Med 75 (Suppl 1): S41, 2014.
6. Pradhan N, Parbin S, Kar S, Das L, Kirtana R, Suma SG, Sengupta D, Deb M, Kausar C and Patra SK: Epigenetic silencing of genes enhanced by collective role of reactive oxygen species and MAPK signaling downstream ERK/Snail axis: Ectopic application of hydrogen peroxide repress CDH1 gene by enhanced DNA methyltransferase activity in human breast cancer. Biochim Biophys Acta Mol Basis Dis 1865: 1651-1665, 2019.
7. Shang F, Lyu Y, Xie XC, Ding BY, Niu J and Wang JJ: RNA-seq analysis of clitea metallica (coleoptera: Chrysomelidae), provides insights into cuticle-related genes and miRNAs. J Econ Entomol 112: 2940-2951, 2019.
8. Maind A and Raut S: Mining conditions specific hub genes from RNA-Seq gene-expression data via biclustering and their application to drug discovery. IET Syst Biol 13: 194-203, 2019.
9. Wu M, Liu Z, Zhang A and Li N: Identification of key genes and pathways in hepatocellular carcinoma: A preliminary bioinformatics analysis. Medicine (Baltimore) 98: e14287, 2019.
10. Pan WY, Zeng JH, Wen DY, Wang JY, Wang PP, Chen G and Feng ZB: Oncogenic value of microRNA-15b-5p in hepatocellular carcinoma and a bioinformatics investigation. Oncol Lett 17: 1695-1713, 2019.
11. Lou W, Liu J, Ding B, Chen D, Xu L, Ding J, Jiang D, Zhou L, Zheng S and Fan W: Identification of potential miRNA-mRNA regulatory network contributing to pathogenesis of HBV-related HCC. J Transl Med 17: 7, 2019.
12. Yin L, Cai Z, Zhu B and Xu C: Identification of key pathways and genes in the dynamic progression of HCC based on WGCNA. Genes (Basel) 9: pii: E92, 2018.

13. Langfelder P and Horvath S: WGCNA: An R package for weighted correlation network analysis. BMC Bioinformatics 9: 559, 2008.
14. Livak KJ and Schmittgen TD: Analysis of relative gene expression data using real-time quantitative PCR and the $2^{-\Delta\Delta Ct}$ method. Methods 25: 402-408, 2001.
15. González-Castro TB, Tovilla-Zárate CA, Genis-Mendoza AD, Juárez-Rojop IE, Nicolini H, López-Narváez ML and Martínez-Magaña JJ: Identification of gene ontology and pathways implicated in suicide behavior: Systematic review and enrichment analysis of GWAS studies. Am J Med Genet B Neuropsychiatr Genet 180: 320-329, 2019.
16. Zhao J, O'Neil M, Vittal A, Weinman SA and Tikhanovich I: PRMT1-dependent macrophage IL-6 production is required for alcohol-induced HCC progression. Gene Expr 19: 137-150, 2019.
17. Machida K, Feldman DE and Tsukamoto H: TLR4-dependent tumor-initiating stem cell-like cells (TICs) in alcohol-associated hepatocellular carcinogenesis. Adv Exp Med Biol 815: 131-144, 2015.
18. Thompson KJ, Humphries JR, Niemeyer DJ, Sindram D and McKillop IH: The effect of alcohol on Sirt1 expression and function in animal and human models of hepatocellular carcinoma (HCC). Adv Exp Med Biol 815: 361-373, 2015.
19. Nischalke HD, Berger C, Lutz P, Langhans B, Wolter F, Eisenhardt M, Kramer B, Kokordelis P, Glassner A, Muller T, *et al*: Influence of the CXCL1 rs4074 A allele on alcohol induced cirrhosis and HCC in patients of European descent. PLoS One 8: e80848, 2013.
20. Chu T, Weng X, Law C, Kong HK, Lau J, Li S, Pham HQ, Wang R, Zhang L, Kao R, *et al*: The ribosomal maturation factor P from Mycobacterium smegmatis facilitates the ribosomal biogenesis by binding to the small ribosomal protein S12. J Biol Chem 294: 372-378, 2019.
21. Lee SJ, Swanson MJ and Sattlegger E: Gcn1 contacts the small ribosomal protein Rps10, which is required for full activation of the protein kinase Gcn2. Biochem J 466: 547-559, 2015.
22. Zhang C, Qie Y, Yang T, Wang L, Du E, Liu Y, Xu Y, Qiao B and Zhang Z: Kinase PIM1 promotes prostate cancer cell growth via c-Myc-RPS7-driven ribosomal stress. Carcinogenesis 40: 202, 2019.
23. Wu Y, Tan X, Liu P, Yang Y, Huang Y, Liu X, Meng X, Yu B, Wu M and Jin H: ITGA6 and RPSA synergistically promote pancreatic cancer invasion and metastasis via PI3K and MAPK signaling pathways. Exp Cell Res 379: 30-47, 2019.
24. Tomioka M, Shimobayashi M, Kitabatake M, Ohno M, Kozutsumi Y, Oka S and Takematsu H: Ribosomal protein uS7/Rps5 serine-223 in protein kinase-mediated phosphorylation and ribosomal small subunit maturation. Sci Rep 8: 1244, 2018.
25. Zhao L, Cao J, Hu K, Wang P, Li G, He X, Tong T and Han L: RNA-binding protein RPS3 contributes to hepatocarcinogenesis by post-transcriptionally up-regulating SIRT1. Nucleic Acids Res 47: 2011-2028, 2019.
26. Mok KW, Mruk DD and Cheng CY: rpS6 regulates blood-testis barrier dynamics through Akt-mediated effects on MMP-9. J Cell Sci 127: 4870-4882, 2014.
27. Tian ZC, Liu GY, Yin H, Luo JX, Guan GQ, Luo J, Xie JR, Shen H, Tian MY, Zheng JF, *et al*: RPS8-a new informative DNA marker for phylogeny of Babesia and Theileria parasites in China. PLoS One 8: e79860, 2013.
28. Liu WJ, Zhou L, Liang ZY, Zhou WX, You L, Zhang TP and Zhao YP: Plasminogen activator inhibitor 1 as a poor prognostic indicator in resectable pancreatic ductal adenocarcinoma. Chin Med J (Engl) 131: 2947-2952, 2018.
29. Chen R, Dawson DW, Pan S, Ottenhof NA, de Wilde RF, Wolfgang CL, May DH, Crispin DA, Lai LA, Lay AR, *et al*: Proteins associated with pancreatic cancer survival in patients with resectable pancreatic ductal adenocarcinoma. Lab Invest 95: 43-55, 2015.
30. Toshimitsu H, Iizuka N, Yamamoto K, Kawauchi S, Oga A, Furuya T, Oka M and Sasaki K: Molecular features linked to the growth-inhibitory effects of gemcitabine on human pancreatic cancer cells. Oncol Rep 16: 1285-1291, 2006.
31. Li TT, Tong AJ, Liu YY, Huang ZR, Wan XZ, Pan YY, Jia RB, Liu B, Chen XH and Zhao C: Polyunsaturated fatty acids from microalgae Spirulina platensis modulates lipid metabolism disorders and gut microbiota in high-fat diet rats. Food Chem Toxicol 131: 110558, 2019.